ELSEVIER

Journal of Alloys and Compounds 271–273 (1998) 400–403

Journal of ALLOYS AND COMPOUNDS

Electrical conductivity of uranium–neptunium mixed oxides

Toshiyuki Yamashita[a,*], Kinji Ohuchi[a], Toshihide Tsuji[b], Tetsuya Kato[b], Manabu Ochida[b], Mitsushige Iwashita[b]

[a]*Department of Chemistry and Fuel Research, Japan Atomic Energy Research Institute, Tokai-mura, Ibaraki 319-11, Japan*
[b]*Department of Nuclear Engineering, Graduate School of Engineering, Nagoya University, Furo-cho, Chikusa-ku, Nagoya 464-01, Japan*

Abstract

The electrical conductivities (σ) of $Np_yU_{1-y}O_{2+x}$ ($y=0.1$ and 0.2) were measured in the range of $10^{-15} \leqslant P_{O_2}$ (Pa) $\leqslant 10^{-1.5}$ at 1273 K and in the temperature range from room temperature to 1273 K for the specimen equilibrated at constant P_{O_2} by the four inserted wires method. Four different dependencies of σ upon P_{O_2} for $Np_yU_{1-y}O_{2+x}$ were observed, similar to the results for UO_{2+x}. Two types of curve were obtained in the log(σ) vs. $1/T$ plots for $Np_yU_{1-y}O_{2+x}$, i.e. L- and Z-shaped curves. Specimens equilibrated at P_{O_2} below $10^{-4.85}$ Pa showed an L-shaped curve, whereas those equilibrated at P_{O_2} between $10^{-4.85}$ and $10^{-2.7}$ Pa showed a Z-shaped one. The activation energy of the electrical conduction for the samples with Z-shaped curves was about 0.3 eV, which was the same value as that of UO_{2+x} in the same P_{O_2} region. From these observations, it is suggested that Np exists as a Np^{4+} ion in these solid solutions and plays no important role on the electrical conduction. © 1998 Elsevier Science S.A.

Keywords: Electrical conductivity; Uranium–neptunium mixed oxides

1. Introduction

Neptunium is the most abundant element among the minor actinides (Np, Am, Cm) in usual spent fuels burned in light water reactors. It is important to understand the fundamental physico-chemical properties of neptunium–uranium mixed oxides, in order to clarify the behavior of Np in the fuel and/or to develop new fuels containing minor actinides. In the preceding papers [1,2], we reported the phase relations of the ternary UO_2–U_3O_8–NpO_2 system and the thermal expansion of $(Np,U)O_2$ solid solutions. We clarified that a wide and homogeneous solid solution phase of $(Np,U)O_{2+x}$ existed in the range of UO_2–$_4O_9$–$U_{0.4}Np_{0.6}O_{2.27}$–NpO_2 and the solid solution phase was almost ideal [1]. From the thermal expansion experiments for the $(Np,U)O_2$ solid solutions by the high-temperature X-ray diffraction method, we found that the linear thermal expansion values of these solid solutions at 1273 K were decreased with increasing Np contents. We also suggested that the heat capacity data of these solid solutions were derived from the thermodynamic relation using these thermal expansion data and literature data with reasonable accuracy [2].

Other important properties are the oxidation state of Np and defect structures in the $(Np,U)O_{2+x}$ solid solutions, which can be estimated through electrical conductivity measurements at high temperatures. We measured the electrical conductivity of $U_{1-y}Pu_yO_{2+x}$ ($y=0.05$, 0.1, 0.2, 0.3, 0.5, 0.9 and 1) [3–5] and clarified the defect structure of these solid solutions. We also obtained information about the oxidation states of U and Pu in these nearly stoichiometric solid solutions, from the analysis of the relation between the electrical conductivity values and Pu contents; some Pu^{3+} and U^{5+} were formed in nearly stoichiometric solid solutions through the charge transfer reaction, $U^{4+}+Pu^{4+}=U^{5+}+Pu^{3+}$ [5]. In the present study, therefore, we measured the electrical conductivity of $(Np,U)O_{2+x}$ solid solutions as a function of the oxygen partial pressures as well as temperatures, in order to obtain information on oxidation states of Np, defect structures and conduction mechanisms in the solid solutions.

2. Experimental details

Neptunium dioxide provided from Fontenay aux Roses, France, was dissolved in conc. HNO_3. After drying the solution, the residue was dissolved in conc. HCl. The solution was purified with an anion exchange resin (DIA-ION SA≠100) in a HCl solution system [6]. Np oxalate

*Corresponding author. Tel.: +81 29 2825496; fax: +81 29 2825935.

0925-8388/98/$19.00 © 1998 Elsevier Science S.A. All rights reserved.
PII S0925-8388(98)00098-X

precipitate was formed by adding oxalic acid to the purified solution and then was decomposed to NpO_2 by heating it at about 1000 K in air. Uranium dioxide was obtained by reducing U_3O_8 in a stream of purified hydrogen gas at 1273 K for 10 h. The U_3O_8 was prepared by oxidizing high-purity uranium metal blocks in air at about 1000 K. Weighed amounts of NpO_2 and UO_2 powders were dissolved in a nitric acid. The mixed solution was gently evaporated and dried up in a mantle heater. The powder of mixed oxide was obtained by calcining the solid nitrate at 1073 K in air.

The oxide powder was subsequently pressed in a 6-mm diameter circular die at about 20 kg mm^{-2}. Four holes of 0.3 mm in diameter were drilled in a straight line, to which 0.3-mm diameter Pt/20%Rh wires were inserted for the use of electrodes. Then, the pellet was sintered in vacuum at 1673 K for 5 h. The electrodes were tightly fixed to the pellet after sintering.

Two electric furnaces for the measurements of the electrical conductivity and oxygen partial pressure were enclosed in a glove box. The electrical conductivity was measured by means of the conventional four inserted wires method as described elsewhere [3–5,7].

The oxygen partial pressure was controlled from 10^{-13} to $10^{-1.5}$ Pa with a CO and CO_2 gas mixture. The oxygen partial pressure was determined from the mixing ratio of the gases and/or by measuring the electrical conductivity of oxygen sensors of barium titanate [8] calibrated in our laboratory. The oxygen sensors were placed before and after the sample to check whether the oxygen partial pressure was controlled exactly. In order to obtain the electrical conductivity data in equilibrium, the samples were held in the same mixed gas atmosphere for periods ranging from 1 to 30 days, depending on the oxygen partial pressure. The activation energy was obtained by the quenching experiment: the sample, which had been equilibrated at 1273 K, was quenched to the desired temperature and its electrical conductivity was measured before the composition of the sample reached equilibrium with the quenched temperature.

3. Results and discussion

The oxygen partial pressure dependencies (P_{O_2}) of the electrical conductivity (σ) of $Np_{0.2}U_{0.8}O_{2+x}$ obtained at 1273 K are shown in Fig. 1, together with those of UO_{2+x} [9], $Pu_{0.2}U_{0.8}O_{2+x}$ [4] and $Th_{0.25}U_{0.75}O_{2+x}$ [10] for comparison. Before the electrical conductivity measurements in the CO/CO_2 mixed gas were initiated, the sample was equilibrated in an 8%H_2/Ar gas atmosphere at 1273 K for 1 week. In the figure, open circles indicate the values of $Np_{0.2}U_{0.8}O_{2+x}$ obtained for increasing oxygen partial pressure, and closed circles indicate decreasing oxygen partial pressure. A small difference is observed in the values for open and closed circles at P_{O_2} below 10^{-7} Pa. The electrical conductivity was recovered to the initial value when the sample was equilibrated in an 8%H_2/Ar gas atmosphere. Therefore it is considered that the electrical conductivity values indicated by open circles are the equilibrium values. A similar behavior had been observed for pure UO_{2+x} at low oxygen partial pressures [9,11]. Although it is not unclear why the electrical conductivity obtained for decreasing oxygen partial pressure is slightly higher than the initial value, some sort of defects or frame of defect structure which are formed at P_{O_2} above 10^{-7} Pa may cause the higher electrical conductivity.

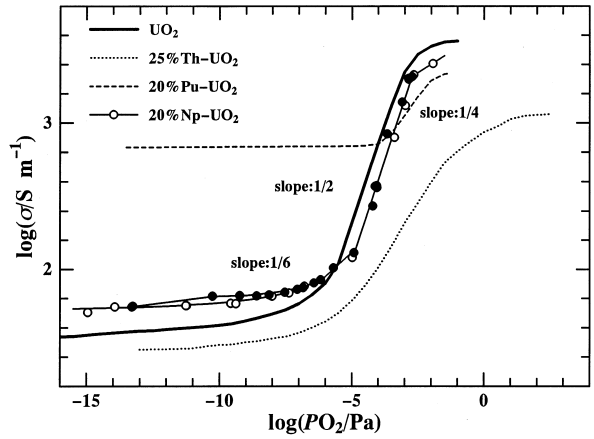

Fig. 1. The oxygen partial pressure dependencies of the electrical conductivity at 1273 K for $Np_{0.2}U_{0.8}O_{2+x}$, UO_{2+x}, $Pu_{0.2}U_{0.8}O_{2+x}$ and $Th_{0.25}U_{0.75}O_{2+x}$. (○,●) $Np_{0.2}U_{0.8}O_{2+x}$. Open symbols indicate the values obtained for increasing oxygen partial pressure, and closed symbols indicate the values for decreasing oxygen partial pressure. A solid line represents the electrical conductivity for UO_{2+x} [9], a broken line that for $Pu_{0.2}U_{0.8}O_{2+x}$ [4] and a dotted line that for $Th_{0.25}U_{0.75}O_{2+x}$ [10].

In Fig. 1, four different dependencies of σ upon P_{O_2} for $Np_{0.2}U_{0.8}O_{2+x}$ are seen.

(1) Above $P_{O_2}=10^{-2.7}$ Pa (region I), the slope of the $\log(\sigma)$ vs. $\log(P_{O_2})$ curve decreases with increasing oxygen partial pressure, presumably owing to the onset of the phase transition from a single-phase MO_{2+x} to a two-phase $MO_{2+x}+M_4O_{9-x}$ region.

(2) Between $P_{O_2}=10^{-4.85}$ and $10^{-2.7}$ Pa (region II), $\log(\sigma)$ increases linearly with increasing $\log(P_{O_2})$, and the slope is almost the same as that for UO_{2+x}.

(3) Between $P_{O_2}=10^{-6.1}$ and $10^{-4.85}$ Pa (region III), $\log(\sigma)$ also increases linearly with increasing $\log(P_{O_2})$, and the slope is smaller than that for region II.

(4) Below $P_{O_2}=10^{-6.1}$ Pa (region IV), the electrical conductivity is independent of P_{O_2}. Closely similar dependencies were also observed for $Np_{0.1}U_{0.9}O_{2+x}$.

From the slopes in regions II and III shown in Fig. 1, the values of n in the relation $\log(\sigma)\propto(1/n)\log(P_{O_2})$ for $Np_{0.2}U_{0.8}O_{2+x}$ were calculated as 1.8 and 6.1, respectively. Those for $Np_{0.1}U_{0.9}O_{2+x}$ were 1.8 and 6.5, respectively. In region II, the formation of the complex defect $\{2(O_i^aO_i^bV_o)\}^{m-}$, similar to the case for undoped UO_{2+x}

[12,13], is represented by $2V_i^a + 2V_i^b + 2O_o + O_2(g) = 2(O_i^aO_i^bV_o)^{m-} + mh^+$,

$$\log(\sigma) \propto \{1/(m+1)\}\log(P_{O_2}) \quad (1)$$

where h^+ is a positive hole and m is the charge of the complex defect. The dependence of $n=1.8$, where $n=m+1$, can be found from Eq. (1) by taking the value $m=1$; the predominant defect for $Np_yU_{1-y}O_{2+x}$ ($y=0.1$ and 0.2) is a singly ionized $\{2(O_i^aO_i^bV_o)\}^-$ which is the predominant defect for UO_{2+x} [12,13] and is a so-called Willis's (2:2:2) type cluster. In region III, where the deviation from the stoichiometry is considered to be small, the formation of another complex defect $(2O_i^aO_i^b2V_o)^{m-}$ is assumed: $2V_i^a + V_i^b + 2O_o + (1/2)O_2(g) = (2O_i^aO_i^b2V_o)^{m-}\} + mh^+$,

$$\log(\sigma) \propto \{1/2(m+1)\}\log(P_{O_2}). \quad (2)$$

The dependence of $n=6.5$ and 6.1 for $y=0.1$ and 0.2, respectively, can be found from Eq. (2) by taking the value $m=2$; the predominant defect for $Np_yU_{1-y}O_{2+x}$ ($y=0.1$ and 0.2) is a doubly ionized $\{2(O_i^aO_i^bV_o)\}^{2-}$, which is the predominant defect for UO_{2+x} [13] and is a so-called Willis's (2:1:2) type cluster.

It is worthwhile to compare the curves of the $\log(\sigma)$ vs. $\log(P_{O_2})$ plots for $(M,U)O_{2+x}$ (M=Th, Np and Pu) shown in Fig. 1. Because the host material for these solid solutions is UO_{2+x}, all the curves are basically considered to be the same trend as that of UO_{2+x}. The curve for $Np_{0.2}U_{0.8}O_{2+x}$ is almost the same as that of UO_{2+x}. The oxygen partial pressure at which a sharp increase in the electrical conductivity begins, shifts slightly to higher P_{O_2} than that of UO_{2+x}, indicating that the oxygen potential of $Np_{0.2}U_{0.8}O_{2+x}$ increases slightly due to the formation of a solid solution between UO_{2+x} and NpO_2. In the curve for $Pu_{0.2}U_{0.8}O_{2+x}$, shown as a broken one, the electrical conductivity at the low P_{O_2} region is much higher than the others. This is due to the increase in carrier concentrations formed through the charge transfer reaction, $U^{4+} + Pu^{4+} = U^{5+} + Pu^{3+}$ [5]. At the high P_{O_2} region, the slope of the $\log(\sigma)$ vs. $\log(P_{O_2})$ plot is 1/4.1, and the predominant defect species is assumed to be a triply ionized $\{2(O_i^aO_i^bV_o)\}^{3-}$ [4]. The curve for $Th_{0.25}U_{0.75}O_{2+x}$ is shown as a dotted one, and the electrical conductivity at the low P_{O_2} region is nearly the same as that of UO_{2+x}, indicating that Th^{4+}, which is considered to be the stable species in this P_{O_2} region, has no important role on the electrical conductivity in the solid solution. At the P_{O_2} region between 10^{-5} and 10^{-2} Pa, the slope of the $\log(\sigma)$ vs. $\log(P_{O_2})$ plot is about 1/4, and Lee [10] proposed a singly charged oxygen interstitial as a predominant defect species. The electrical conductivity keeps increasing up to about $P_{O_2}=10^2$ Pa, which is a great contrast to the others, suggesting that a wide two-phase region of $MO_{2+x} + M_4O_{9-y}$ exists in the ThO_2–UO_{2+x} system.

Some typical examples of the plots of $\log(\sigma T)$ against the reciprocal temperature for the $Np_yU_{1-y}O_{2+x}$ ($y=0.1$ and 0.2) samples quenched after annealing at 1273 K under $P_{O_2}=10^{-2.85}$ (region II) and $10^{-9.15}$ Pa (region III) are shown in Fig. 2. The measured electrical conductivities of all samples were reversible for increasing (indicated by open symbols) and decreasing (indicated by closed symbols) temperature, indicating that no compositional change took place during the measurements. As seen in the Fig. 2, two different dependencies of $\log(\sigma T)$ on $1/T$ are observed:

(1) samples equilibrated at 1273 K under P_{O_2} between $10^{-4.85}$ and $10^{-2.7}$ Pa (region II), where the deviation of composition from the stoichiometry seems to be large, show Z-shaped curves;

(2) samples equilibrated at 1273 K under P_{O_2} below $10^{-4.85}$ Pa (regions III and IV), where the composition is considered to be nearly stoichiometric, show L-shaped curves.

Because there were few data points for the high temperature region of these curves, the activation energies of electrical conduction were not obtained.

The activation energies of electrical conduction for $Np_yU_{1-y}O_{2+x}$ ($y=0.1$ and 0.2) with Z-shaped behavior were calculated from the slope in the temperature range above the high temperature break points in Fig. 2. Fig. 3 shows the activation energies of $Np_yU_{1-y}O_{2+x}$ ($y=0.1$ and 0.2) samples obtained in region II as a function of y, together with the previous results of UO_{2+x} [9], $Pu_yU_{1-y}O_{2+x}$ ($y=0.05$–0.3) [4,5] and $La_y(Pu_{0.2}U_{0.8})_{1-y}O_{2+x}$ ($y=0.01$ and 0.1) [14] by the present authors. As can be seen from Fig. 3, the activation energies of electrical conduction for $Np_yU_{1-y}O_{2+x}$ do not depend on Np contents, and are an almost constant value of 0.3 eV, which is the same value as that of UO_{2+x}. On the

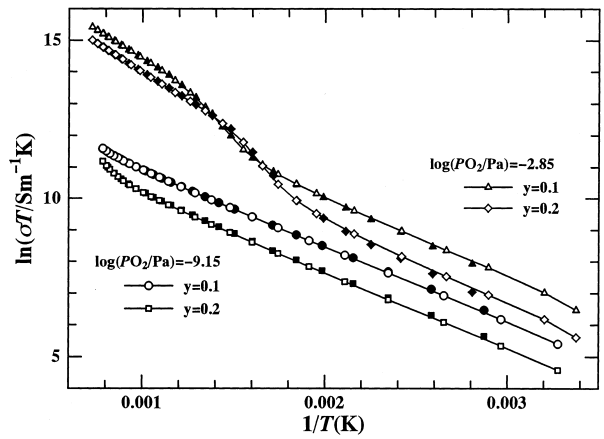

Fig. 2. The typical relations between $\log(\sigma T)$ and $1/T$ for the $Np_yU_{1-y}O_{2+x}$ ($y=0.1$ and 0.2) samples quenched after annealing at 1273 K under oxygen partial pressure of $10^{-2.85}$ and $10^{-9.15}$ Pa. (△,▲) $y=0.1$, $P_{O_2}=10^{-2.85}$ Pa; (◊,♦) $y=0.2$, $P_{O_2}=10^{-2.85}$ Pa; (○,●) $y=0.1$, $P_{O2}=10^{-9.15}$ Pa; (□,■) $y=0.2$, $P_{O_2}=10^{-9.15}$ Pa. Open symbols indicate the values obtained for increasing temperature and closed symbols for decreasing temperature.

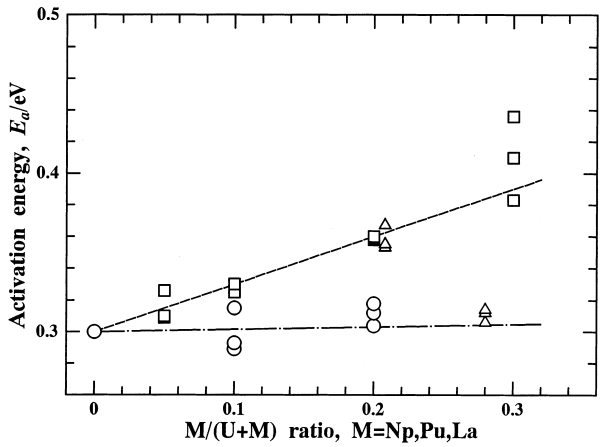

Fig. 3. Relation between the activation energy of the electrical conduction and the value of M/(M+U) (M=Np, Pu and La) ratio. (○) $Np_yU_{1-y}O_{2+x}$, (□) $Pu_yU_{1-y}O_{2+x}$ [4,5], (△) $La_y(Pu0.2U0.8)_{1-y}O_{2+x}$ [14].

contrary, the activation energies for $Pu_yU_{1-y}O_{2+x}$ increase linearly with increasing Pu contents. The 1% La-doped $Pu_{0.2}U_{0.8}O_{2+x}$ has an activation energy of about 0.36 eV which is on the line for $Pu_yU_{1-y}O_{2+x}$, whereas the value for 10% La-doped $Pu_{0.2}U_{0.8}O_{2+x}$ decreases to about 0.31 eV which is on the line for $Np_yU_{1-y}O_{2+x}$. These observation can be explained as follows. The activation energy of holes formed from the complex defect formation reaction (Eq. (1)) or by doping a large amount of La^{3+} is considered to be a constant of about 0.3 eV. In $Pu_yU_{1-y}O_{2+x}$ solid solutions, on the other hand, some sort of interaction between U^{4+} and Pu^{4+}, such as the charge transfer reaction $U^{4+}+Pu^{4+}=U^{5+}+Pu^{3+}$, causes the increase of the activation energy with increasing Pu contents, and the introduction of a small amount of holes by doping La^{3+} into the solid solution does not affect the interaction very much.

4. Conclusions

The electrical conductivities of $Np_yU_{1-y}O_{2+x}$ ($y=0.1$ and 0.2) have been measured both as a function of oxygen partial pressure and temperature. Four different dependencies upon oxygen partial pressure were observed, similar to the results for UO_{2+x}. In the P_{O_2} regions of $10^{-4.85}$ to $10^{-2.7}$ Pa, and $10^{-6.1}$ to $10^{-4.85}$ Pa, a linear relationship of $\log(\sigma)$ vs. $\log(P_{O_2})$ plots were observed. The predominant defect species were determined to be a singly ionized complex defect of $\{2(O_i^aO_i^bV_o)\}^-$ for the former region, and a doubly ionized complex defect of $(2O_i^aO_i^b2V_o)^{2-}$ for the latter region, from the slope of the $\log(\sigma)$ vs. $\log(P_{O_2})$ plots.

Two types of curve were observed for the $\log(\sigma)$ vs. $1/T$ plots for these solid solutions; an L-shaped curve and a Z-shaped one. The L-shaped curves were observed for the samples equilibrated at 1273 K under P_{O_2} below $10^{-4.85}$ Pa, whereas the Z-shaped ones were observed for those equilibrated under P_{O_2} between $10^{-4.85}$ and $10^{-2.7}$ Pa. The activation energy of the electrical conduction for the samples with Z-shaped curves was about 0.3 eV, which was the same value of that of UO_{2+x} in the same P_{O_2} region.

From the results obtained in the present investigation, it is suggested that Np exists as a Np^{4+} ion in these solid solutions and plays no important role on the electrical conduction.

References

[1] T. Yamashita, N. Nitani, K. Ohuchi, T. Muromura, T. Tsuji, H. Inagaki, T. Kato, J. Alloys Comp. 213–214 (1994) 375.
[2] T. Yamashita, N. Nitani, T. Tsuji, T. Kato, J. Nucl. Mater. 247 (1997) 90.
[3] K. Naito, T. Tsuji, K. Ohuchi, T. Yahata, T. Yamashita, H. Tagawa, J. Nucl. Mater. 95 (1980) 181.
[4] K. Naito, T. Tsuji, T. Fujino, T. Yamashita, J. Nucl. Mater. 169 (1989) 329.
[5] T. Fujino, T. Yamashita, K. Ohuchi, K. Naito, T. Tsuji, J. Nucl. Mater. 202 (1993) 154.
[6] M. Izumo, T. Sorita, K. Hata, T. Sekine, H. Matsuoka, R. Motoki, S. Baba, private communication.
[7] T. Ishii, K. Naito, K. Oshima, J. Nucl. Mater. 35 (1970) 335.
[8] K. Naito, T. Tsuji, S. Watanabe, H. Sakai, Solid State Ionics 3–4 (1981) 635.
[9] T. Yamashita, K. Ohuchi, T. Fujino, K. Naito, T. Tsuji, unpublished work.
[10] H.M. Lee, J. Nucl. Mater. 48 (1973) 107.
[11] N.J. Dudney, R.L. Coble, H.L. Tuller, J. Am. Ceram. Soc. 64 (1981) 627.
[12] T. Matsui, K. Naito, J. Nucl. Mater. 132 (1985) 212.
[13] A. Nakamura, T. Fujino, J. Nucl. Mater. 140 (1986) 113.
[14] T. Tsuji, K. Naito, T. Yamashita, T. Fujino, J. Alloys Comp. 213–214 (1994) 378.